Desalination and Water Treatment
www.deswater.com
doi: 10.5004/dwt.2023.29443

290 (2023) 71–81
April

Comparison of Cd(II) adsorption performance on two phosphate modified straw biochar

Tianqi Tao

School of Civil Engineering, Architecture and Environment, Hubei University of Technology, Wuhan 430068, China, email: 101910677@hbut.edu.cn

Received 6 November 2022; Accepted 1 March 2023

ABSTRACT

Phosphate-modified biochar is a good material for the heavy metals removal from wastewater. However, different phosphate modified straw biochar have dissimilar adsorption performance for heavy metals. In this work, Na_3PO_4-modified straw biochar (PBC) and Na_2HPO_4-modified straw biochar (SPBC) were used to remove Cd(II) from aqueous solution. Moreover, the effects of dosage, solution pH, coexisting ions, adsorption time, temperature and initial concentration on the Cd(II) removal by the sorbent were investigated. The result shown that SPBC possessed richer pore structure and O-containing functional groups. The adsorption experiments indicated that the optimum adsorption performance could be obtained at pH = 6.0 and dosage 25 mg. K^+, Na^+, Ca^{2+} and Mg^{2+} had little effect on the removal of Cd(II) by biochar, while Cu^{2+} and Pb^{2+} had strong inhibitory effect. Notably, SPBC reached the time of adsorption equilibrium much faster than biochar (BC) and PBC. The pseudo-second-order kinetic model and Langmuir model could describe the adsorption process of Cd(II) well. The theoretical maximum adsorption capacities of BC, PBC and SPBC for Cd(II) were 54.55, 114.79 and 154.13 mg/g at 25°C, respectively. The removal mechanisms included complexation, ion exchange, Cd(II)-π interaction, electrostatic interaction and co-precipitation. This work suggested that Na_2HPO_4-modified straw biochar held greater potential to remove Cd(II) from wastewater than Na_3PO_4-modification.

Keywords: Straw biochar; Phosphate-modification; cadmium (Cd(II)); Adsorption performance comparison; Mechanism

1. Introduction

In recent years, cadmium (Cd(II)) pollution has caused a great deal of concern. Cd(II) can cause a variety of health problems in humans, including neurological disorders, kidney failure, eardrum disease and cancer [1–3]. There are relatively strict restrictions on Cd(II) emissions around the world. Therefore, it is of great significance to develop effective Cd(II) removal technology in water.

Adsorption is one of the most commonly used techniques for Cd(II) removal from water due to its high efficiency, simple operation and low cost [3–6]. Biochar is a carbon material synthesised by pyrolysis of biomass material under oxygen-limited conditions [7–11]. Recent studies have shown that biochar has good affinity for heavy metal removal due to its porous structure and aromatic surface [12–14]. However, the original biochar has a limited specific surface area and fewer surface active sites, resulting in poor adsorption capacity [15,16]. Chemical modification can significantly improve the adsorption capacity of biochar by improving the pore structure and chemical activity [17]. For example, biochar show good adsorption performance after modification with $KMnO_4$, H_3PO_4 and Fe_3O_4 [2,7,18]. However, these modification methods may cause severe corrosion damage to the production equipment or release metal ions during the adsorption, leading to secondary

pollution [19]. Therefore, it is necessary to develop a new environmentally friendly and efficient biochar modification method [20]. Sodium phosphate has no strong corrosiveness, reducing the loss of production equipment [21]. Phosphate modification is an important method to improve the adsorption capacity of biochar for heavy metals [7]. The method has the advantages of low cost, good effect and no secondary pollution. Previous literature has shown that phosphate-modified biochar materials have a good adsorption effect on heavy metals in water because Cd(II) phosphate compounds are more insoluble than other salt forms [22]. In addition, phosphorus modified biochar can increase the number of surface functional groups, pores and specific surface area, thereby improving the adsorption capacity of biochar [7]. However, different phosphate modified biochar have different adsorption properties for Cd(II). Therefore, two phosphate-modified biochars were used to remove Cd(II) from aqueous solution. Miao and Li [21] shown that the adsorption capacity of Pb(II) by KH_2PO_4 modified straw biochar was 4.15 times higher than that of the original biochar. Additionally, the adsorption capacity of Pb(II), Cu(II), and Cd(II) by bamboo wood chip biochar activated by guanidine phosphate was 166.2, 81.7, and 60.3 mg/g, respectively [23]. Peanut shell biochar was modified with ammonium polyphosphate (PABC), phosphoric acid (PHBC) and ammonium dihydrogen phosphate (PNBC). The maximum adsorption capacities of PABC, PHBC and PNBC for Cd(II) were 155, 138 and 99 mg/g, respectively, which were 4.84, 4.32 and 3.10 times higher than those of the original biochar [7]. The above studies indicated that phosphate-modified biochar had huge potential for removing heavy metals from aqueous solution. To our knowledge, no literature had been done for the time being to compare the adsorption performance of Na_3PO_4 and Na_2HPO_4 modified rice straw biochar for Cd(II).

In this work, rice straw was used as feedstock for biochar preparing. Na_3PO_4 and Na_2HPO_4 were selected for biochar modification. The objectives of this work were: (1) to compare the Cd(II) adsorption performance of modified biochar; (2) to investigate the Cd(II) adsorption behaviour on biochar; and (3) to analyse the adsorption mechanism on modified biochar.

2. Materials and methods

2.1. Preparation of biochar

2.1.1. Preparation of biochar

The rice straw was taken from a farmland in Wuhan (Hubei Province, China) and dried in a oven (DF205, Electric Equipment Technology Co., Ltd., China) at 80°C to a constant weight. The dried straw was crushed by ball mill and the straw powder was collected. 50 mg straw powder was added to the crucible and pyrolyzed in a muffle furnace at 600°C in a N_2 atmosphere for 2 h. The black solid was biochar and recorded as BC.

2.1.2. Preparation of modified straw biochar

BC and phosphate solids were added to a 200 mL solution at a mass ratio of 1:1, and the pH was adjusted to 11.0 using 0.1 mol/L NaOH solution. The solution was stirred in water bath at 80°C for 2 h at 150 rpm. The reactants were collected by filtration and dried in a 60°C oven for 12 h. The $Na_3PO_4^-$ and Na_2HPO_4-modified biochar were recorded as PBC and SPBC, respectively.

2.2. Batch adsorption experiments

25 mL of 50 mg/L Cd(II) solution were added to centrifuge tube (50 mL) and the pH was adjusted using 0.1 mol/L HNO_3 and NaOH solution. Add a quantity of BC to the solution. The centrifuge tube was adsorbed in 150 rpm shaker (IS-RDD3, Crystal Technology & Industries, USA) at 25°C for 600 min. The effects of the dosage (5~50 mg), initial pH (2.0~9.0) and co-existing ions (K^+, Na^+, Ca^{2+}, Mg^{2+}, Cu^{2+} and Pb^{2+}) on biochars in removing Cd(II) were investigated. 1 g/L biochar and 50 mg/L Cd(II) solution were added to centrifuge tube. The tube was placed in a shaker at 25°C and 150 rpm for 10~600 min to investigate the effect of adsorption time on Cd(II) removal. 1 g/L biochar and different concentrations (50~300 mg/L) of Cd(II) solution mixed, and placed in shaker at 150 rpm and 25°C to investigate the effect of concentration on Cd(II) removal.

Every experiment was repeated three times and the average value was used as the determination value. The solution was filtered through 0.22 μm filter membrane and the Cd(II) concentration in the filtrate was determined by atomic absorption spectrophotometry (AA-6300, Shimadzu, Japan). The removal efficiency [Eq. (1)] and adsorption capacity [Eq. (2)] were calculated.

$$R = \frac{C_0 - C_e}{C_0} \times 100\% \tag{1}$$

$$q_e = \frac{\left(C_0 - C_e\right)V}{m} \tag{2}$$

where R is the removal efficiency, %; C_0 is the initial Cd(II) mass concentration in solution, mg/L; C_e is the Cd(II) mass concentration in solution after adsorption equilibrium, mg/L; q_e is the equilibrium adsorption capacity, mg/g; V/m is the ratio of solution volume to adsorbent mass, mL/mg.

2.3. Adsorption kinetics and isotherms

Adsorption kinetics: the pseudo-first-order model [Eq. (3)], the pseudo-second-order model [Eq. (4)], Elovich model [Eq. (5)] and the intraparticle diffusion model [Eq. (6)] were used for fitting analysis.

$$q_t = q_e\left(1 - e^{-k_1 t}\right) \tag{3}$$

$$q_t = \frac{q_e^2 k_2 t}{1 + q_e k_2 t} \tag{4}$$

$$q_t = \frac{1}{\beta}\ln\left(\alpha\beta t\right) \tag{5}$$

$$q_t = K_d t^{1/2} + C_i \quad (6)$$

where q_e and q_t are the adsorption capacity at the equilibrium time and time "t" time (mg/g), respectively; k_1 and k_2 represent adsorption rate constant of the pseudo-first-order (min^{-1}) and the pseudo-second-order (g/mg·min), respectively; α and β are the initial absorbance (mg/g·min) and desorption constant (g/mg), respectively; K_d is the intraparticle diffusion rate constant (mg/m·$min^{1/2}$); C_i is the boundary layer constant.

Adsorption isotherms: The Langmuir isotherm model [Eq. (7)], the Freundlich isotherm model [Eq. (8)], and Temkin isotherm [Eq. (9)] were used to fit these date.

$$q_e = \frac{q_{\max} K_L C_e}{1 + K_L C_e},\ R_L = \frac{1}{1 + K_L C_0} \quad (7)$$

$$q_e = K_f C_e^{1/n} \quad (8)$$

$$q_e = \frac{RT}{b_T} \ln\left(A_T C_e\right) \quad (9)$$

where q_e is the adsorption capacity at equilibrium (mg/g); C_e is the concentration of Cd(II) at adsorption equilibrium (mg/L); q_{max}, K_L and R_L are the maximum adsorption capacity of Cd(II) (mg/g), Langmuir equilibrium constant (L/mg) and separation factor, respectively; K_f and n represent the Freundlich affinity coefficient ($mg^{1-n}·L^n/g$) and Freundlich constant related to the surface site heterogeneity, respectively; A_T (1/g) and b_T (kJ/mol) are Temkin constants; R is the global constant of gases, and T is the absolute temperature (K).

The chi-square test and hybrid fraction was used to check how well the model fits [9]. Small χ^2 value and hybrid fraction indicated its similarities while a larger number represents the variation of the experimental data.

The thermodynamic investigation of Cd(II) removal at different temperatures (288, 298 and 308 K). The thermodynamic parameters for the removal process were calculated using Eqs. (10) and (11), and the relevant parameters are listed in Table 5.

$$\ln K^\circ = \frac{\Delta S^\circ}{R} - \frac{\Delta H^\circ}{RT} \quad (10)$$

$$\Delta G^\circ = -RT \ln K^\circ \quad (11)$$

where R is the gas constant (8.314 kJ/mol). $K°$ is the equilibrium constant and T is the Kelvin temperature (K). The $\Delta G°$, $\Delta H°$ and $\Delta S°$ represent the standard free energy (kJ/mol), enthalpy (J/mol), and entropy (J/mol), respectively. The values of $\Delta H°$ and $\Delta S°$ were calculated from the slope and intercept of the linear regression curve of $\ln K°$ vs. $1/T$.

2.4. Representation analysis

The surface morphology of biochar was examined using a scanning electron microscopy (MERLIN, Carl Zeiss AG, Germany). The surface functional groups of biochar were measured with Fourier-transform infrared spectroscopy (FTIR, CCR-1, Thermo-Nicolet, USA) by using the KBr disk technique. The phase compositions of biochar were determined through power X-ray diffraction (XRD, D8, Bruker, Germany) with Cu Kα radiation over the 2θ range of 10°~70°. The zeta potentials of biochar were measured in the solution by Zetasizer Nano Analyzer (Zetasizer 3000HS, Malvern, UK). The Specific surface area and total pore volume of biochar were investigated with N_2 adsorption–desorption measurements at 77 K using Brunauer–Emmett–Teller analyser (Gemini VII 2390 V1.03, Micromeritics Instrument Corp., USA).

2.5. Adsorption–desorption experiments

After adsorption, the adsorbed biochar was centrifuged and shaken in 0.1 mol/L HCl for 2 h. Afterwards, biochar after desorption washed with distilled water and dried at 60°C. The obtained biochar continued for adsorption experiments. The Cd(II) removal efficiency after each adsorption experiment was calculated.

3. Results and discussion

3.1. Characterisation of biochars

The S_{BET}, volume and pore size of the modified biochar increased. SPBC held largest specific surface area (358.49 m^2/g), pore volume (0.387 cm^3/g) and pore size (10.47 nm). This indicated that the phosphate-modified biochar effectively improved the pore structure, which facilitated the pollution removal by the biochar. Additionally, this result indicated that Na_2HPO_4-modified biochar can be more beneficial to ameliorate of biochar pore structure. The element analysis showed that the C content of the biochar decreased from 85.68% to 68.18% and 65.48%, while the total O content increased from 8.49% to 12.57% and 15.64%. This indicated that the modification was effective in increasing the amount of O-containing groups in the biochar. Previous literature shown that complexation between O-containing groups and Cd was an important way of removal [24,25]. In contrast, there was little change in the content of H and N. The P increased from 1.48% to 6.91% and 7.19%, indicating that the phosphate modified biochar increased the amount of P in the biochar. Furthermore, the pH_{zpc} of BC, PBC and SPBC were 4.97, 4.32 and 4.48, respectively.

As shown in Fig. 1, the surface of BC was uneven and there was a relatively regular pore structure. The surface void structure was not very developed, which was consistent with its small specific surface area. After phosphate modification, the regular pores on the surface of biochar were destroyed, which facilitated the adsorption of pollutants. The surface structure of SPBC was more broken, indicating that Na_2HPO_4 was more conducive to improving the pore structure. This result was also consistent with the specific surface area analysis.

3.2. Dosage

Fig. 1a shown the effect of dosage on the Cd(II) removal. When the dosage was increased from 5 mg to 25 mg, the Cd(II) removal efficiency by BC, PBC and SPBC increased

from 11.25%, 21.06% and 32.05% to 48.35%, 75.84% and 96.59%, respectively. This was attributed to the biochar provided more adsorption sites. The Cd(II) removal efficiency increased slowly when the dosage was higher than 25 mg. This was due to the limited amount of Cd(II) in the aqueous solution and the vast majority of Cd(II) was removed. Additionally, previous literature suggested that excessive adsorbent caused agglomeration and discouraged the contaminants adsorption [25]. Nevertheless, the adsorption capacity of Cd(II) adsorbed by the sorbent gradually decreased as the dosage was increased from 5 to 50 mg. The decrease in adsorption capacity of Cd(II) was due to a limited concentration of Cd(II) in solution, which can result in a decrease in adsorption capacity per unit area [26]. Therefore, the optimum dosage was chosen to be 25 mg, taking into account the removal efficiency and economic efficiency.

3.3. Initial pH

The effect of solution pH on the Cd(II) removal is shown in Fig. 2b. The removal efficiency and adsorption capacity increased as pH increased to 6.0, reaching a stability at pH 6.0~9.0. At pH 6.0, the removal efficiency of Cd(II) by BC, PBC and SPBC reached 48.15%, 75.62% and 96.87%, respectively. Moreover, the Cd(II) adsorption capacity of BC, PBC and SPBC was 24.08, 37.81 and 48.44 mg/g at pH 6.0, respectively. Typically, the zeta potential value represents the surface electrical properties of the sorbent. As shown in Table 1, the zero potential points (pH_{zpc}) for BC, PBC and SPBC were 4.97, 4.32 and 4.48, respectively. This indicated that when the pH solution was below pH_{zpc}, the adsorbent surface was positively charged and vice versa [9,27]. This was attributed to the electrostatic repulsion between the positively charged biochar and the positively charged Cd(II) at lower pH [28,29]. As the pH increased, the biochar surface became progressively more negatively charged and electrostatically attracted to positively charged Cd(II). Additionally, a large amount of H^+ in solution competed with Cd(II) for adsorption sites on the biochar at low pH. pH increased, and the H^+ concentration in solution decreased and the competition with Cd(II) diminished [24]. The mechanism of Cd(II) removal included electrostatic attraction.

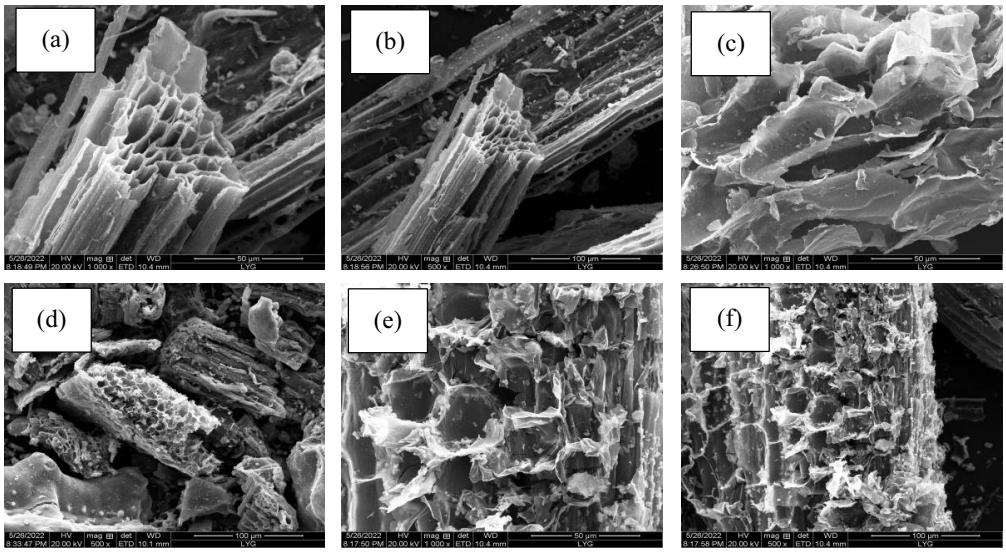

Fig. 1. Scanning electron microscopy analysis of BC (a, b), PBC (c, d) and SPBC (e, f).

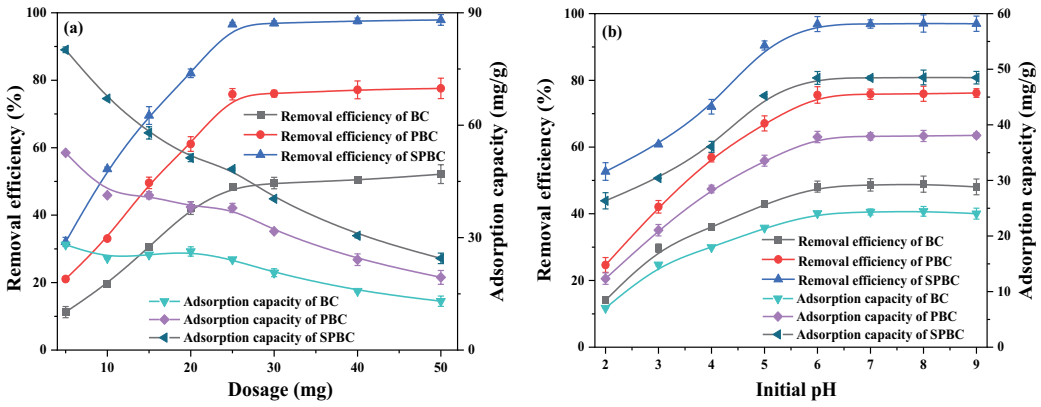

Fig. 2. Effect of dosage (a) and initial pH (b) on sorbent for Cd(II) adsorption (T = 25°C, C_0 = 50 mg/L, and contact time = 600 min).

3.4. Coexisting ions

The presence of K^+, Na^+, Ca^{2+} and Mg^{2+} had little effect on the Cd(II) adsorption (Fig. 3a and b). However, the Pb^{2+} and Cu^{2+} caused the removal efficiency and adsorption capacity decreased. Of these, the Pb^{2+} had significant effect on the adsorption, followed by Cu^{2+}. It was speculated that there was competitive adsorption between Cd(II) and Cu^{2+} or Pb^{2+}. It was also possible that the affinity of biochar for Cu^{2+} or Pb^{2+} was higher than that of Cd(II), resulting in obvious inhibition of Cd(II) removal [30].

3.5. Adsorption–desorption experiment

The adsorption–desorption experiments were investigated at solution pH of 6.0, dosage of 25 mg, concentration of 50 mg/L, adsorption time of 600 min and temperature of 25°C. The results of the five adsorption–desorption experiment showed that the removal efficiency of BC and PBC decreased to 23.61% and 65.29%, while the removal efficiency of SPBC maintained above 90%. After 5 adsorption–desorption experiments, the adsorption capacity of BC, PBC and SPBC was 11.81, 32.65 and 45.54 mg/g, respectively. This indicated that the Na_2HPO_4-modified biochar possessed better regeneration capacity, suggesting that SPBC held the potential to be better applied for the Cd(II) removal from wastewater.

3.6. Adsorption kinetics

From Fig. 4a, the Cd(II) removal process was roughly divided into three stages. The first stage was the rapid adsorption stage (10~60 min), in which the adsorption capacity of Cd(II) by BC, PBC and SPBC increased rapidly from 2.99, 13.25 and 25.10 mg/g to 15.75, 29.58 and 44.29 mg/g, respectively. The second stage was the slow adsorption stage, in which the adsorption capacity of Cd(II) by BC, PBC and SPBC increased slowly to 22.51, 37.03 and 48.62 mg/g, respectively. The third stage was the adsorption stage. The faster

Table 1
Characteristics analysis of biochars

	S_{BET} (m^2/g)	Volume (cm^3/g)	Pore size (nm)	C (%)	H (%)	O (%)	N (%)	P (%)	pH_{zpc}
BC	124.91	0.154	3.72	75.68	1.28	8.49	0.29	1.48	4.97
PBC	307.48	0.361	9.45	68.18	1.34	12.57	0.37	6.91	4.32
SPBC	358.47	0.387	10.47	65.48	1.36	15.64	0.33	7.19	4.48

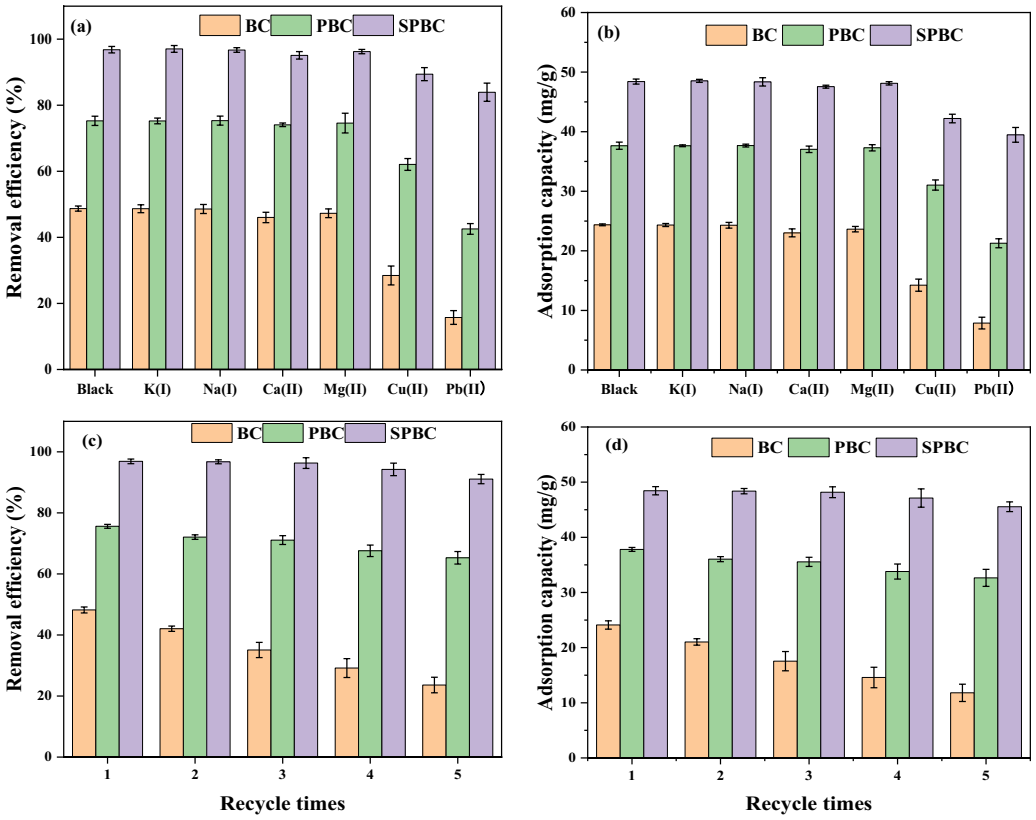

Fig. 3. Effect of coexisting ions (a, b) and adsorption–desorption experiment (c, d) on the Cd(II) removal (T = 25°C, dosage = 25 mg, pH = 6.0, C_0 = 50 mg/L, and contact time = 600 min).

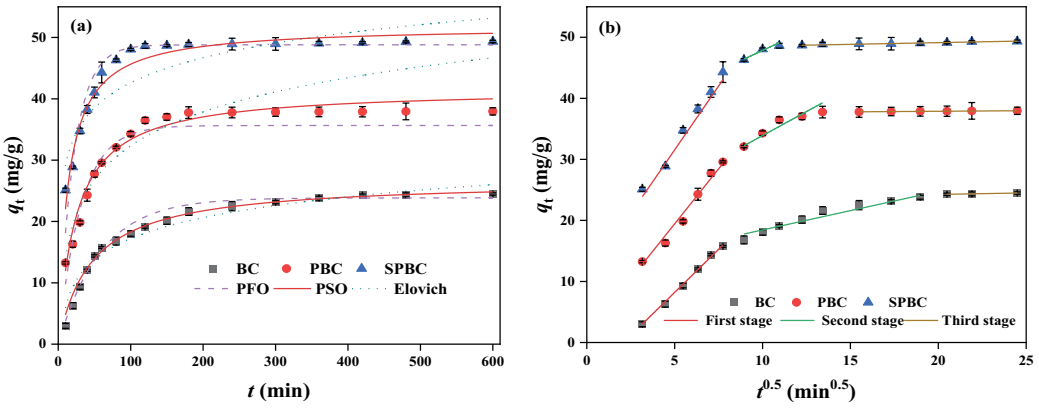

Fig. 4. Pseudo-first-order, pseudo-second-order, Elovich (a) and intraparticle diffusion (b) model fitting curve on the Cd(II) removal (T = 25°C, dosage = 25 mg, pH = 6.0, and C_0 = 50 mg/L).

adsorption in the initial stage was due to the presence of a large number of adsorption sites on the adsorbent surface, which decreased as the adsorption time increases, leading to a slower increase and reaching equilibrium [31,32]. Additionally, the Cd(II) adsorption capacity by SPBC was consistently higher than that of BC and PBC, presumably due to the rich O-containing groups of SPBC [33]. Notably, SPBC (120 min) reached the time of adsorption equilibrium much faster than BC (420 min) and PBC (300 min).

As shown in Table 2, the correlation coefficients of the pseudo-first-order kinetic model and Elovich model were smaller than those of the pseudo-second-order kinetic model, indicating that the pseudo-second-order kinetic model can more accurately describe the Cd(II) adsorption process [34]. This result indicated that the Cd(II) removal process could be chemisorption [2,7]. The smaller value of the k_2 indicated that the adsorption rate was proportional to the number of adsorption sites [35]. Moreover, the theoretical adsorption capacity ($q_{e,cal}$) of the pseudo-second-order kinetic model was closer to the actual adsorption capacity ($q_{e,exp}$), which also indicated that the pseudo-second-order kinetic model was more suitable to describe the Cd(II) removal [9,10]. As shown in Fig. 4b, the intraparticle diffusion model divided the adsorption process into three stages. The first stage was the entry of Cd(II) from the solution to the biochar surface [22,30]. The second stage was the diffusion of Cd(II) from the surface to the pores inside, the third stage was the adsorption equilibrium stage [2,36]. Additionally, the intraparticle diffusion constants $K_{d1} > K_{d2} > K_{d3}$ and the boundary layer constants $C_1 < C_2 < C_3$ indicated that the first diffusion stage dominated the adsorption process [8,20].

Table 2
Kinetic model parameters of Cd(II) adsorption

	BC	PBC	SPBC
$q_{e,exp}$ (mg/g)	24.49	37.96	49.34
Pseudo-first-order			
$q_{e,cal}$ (mg/g)	22.85	34.65	46.80
k_1 (min^{-1})	0.017	0.032	0.046
R^2	0.979	0.943	0.927
Pseudo-second-order			
$q_{e,cal}$ (mg/g)	25.13	39.65	50.82
k_2 (g/mg·min)	0.813 × 10^{-3}	0.965 × 10^{-3}	1.420 × 10^{-3}
R^2	0.990	0.976	0.959
Elovich			
α (mg/g·min)	6.673	47.284	565.133
β (g/mg)	0.182	0.152	0.171
R^2	0.901	0.899	0.785
Intraparticle diffusion			
C_1	–5.90	1.43	10.66
K_{d1} (mg/m·min$^{1/2}$)	2.822	3.602	4.181
R_1^2	0.995	0.991	0.953
C_2	12.11	18.16	34.47
K_{d2} (mg/m·min$^{1/2}$)	0.633	1.573	1.337
R_2^2	0.977	0.941	0.930
C_3	23.25	37.50	48.01
K_{d3} (mg/m·min$^{1/2}$)	0.050	0.019	0.056
R_3^2	0.998	0.956	0.978

3.7. Adsorption isotherm

The effect of the initial Cd(II) concentration (50~300 mg/L) and the adsorption temperature (15°C, 25°C and 35°C) was investigated. As shown in Fig. 5, the Cd(II) adsorption capacity increased rapidly and then reached stability. To analyse the Cd(II) removal process by biochar, the experimental data were fitted by the Langmuir model [Eq. (6)], Freundlich model [Eq. (7)] and Temkin model [Eq. (8)]. As shown in Table 3, the relationship of the fit coefficients was Langmuir > Freundlich and Temkin, which implied that the Langmuir model was a better account of the Cd(II) adsorption [29,32,37]. Moreover, both χ^2 and hybrid fraction of the Langmuir isotherm model were smaller than those of the Freundlich and Temkin models, suggesting that the Langmuir model can better describe the process of Cd(II) removal by biochars [9,10]. This also suggested that the Cd(II) adsorption was a single and homogeneous adsorption process [4,7,38]. Notably, the maximum adsorption capacity

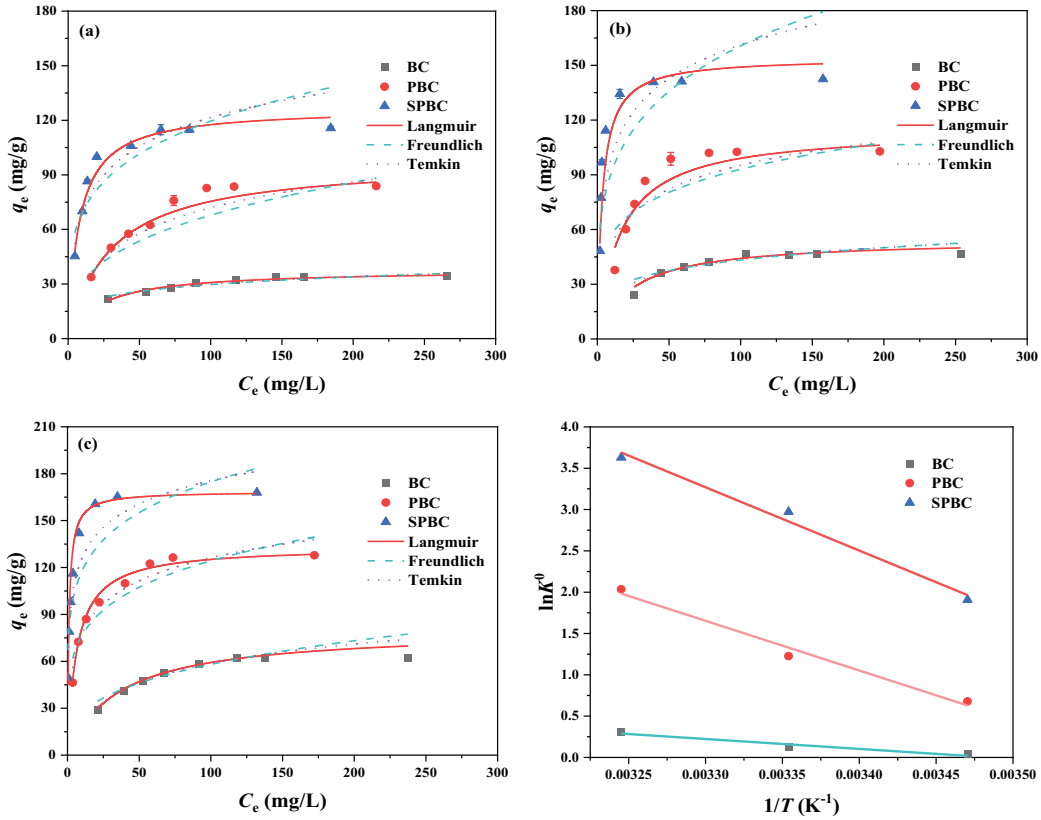

Fig. 5. Isothermal model fitting of Cd(II) adsorption (a) and plot of ln$K°$ vs. 1/T for the estimation of thermodynamic parameters (b) (dosage = 25 mg, pH = 6.0, and contact time = 600 min).

of sorbent for Cd(II) was found at 35°C, indicating that the temperature increase favoured the Cd(II) removal by sorbent [27]. Additionally, the maximum adsorption capacities of 54.41, 122.13 and 149.28 mg/g for BC, PBC and SPBC at 25°C, respectively, indicated that SPBC had better ability to remove Cd(II). Furthermore, SPBC had smaller partition coefficient R_L compared to PBC and BC, which indicated that SPBC possessed higher affinity for Cd(II) [8,13]. In Table 4, the adsorption capacity of biochar for Cd(II) with different modified biochar was compared. The results demonstrated that the q_{max} of Cd(II) by SPBC was higher than that of $KMnO_4$-modified biochar [39], sulfide-iron decorated biochar [40], guanidine phosphate-modified biochar [23], Fe_3O_4-modified biochar [18] and K_3PO_4-modified biochar [35], indicating that SPBC held the potential to remove Cd(II) from aqueous solution.

Thermodynamic analysis was displayed in Table 5. The negative $\Delta G°$ indicated that the Cd(II) removal was spontaneous behaviour [10]. Additionally, the positive $\Delta H°$ indicated that the adsorption reaction was heat process [9]. $\Delta S° > 0$ indicated an increase in the disorder of the solid–liquid phases during the interaction [9,10,27].

3.8. Adsorption mechanism analysis

To explore adsorption mechanism, functional group changes before and after adsorption analyzed by FTIR. The characteristic peaks in BC were –OH (3,423 cm^{-1}), C=O/C=C (1,628 cm^{-1}), C–O (1,076 cm^{-1}) and P–O/P=O (709 and 603 cm^{-1}) [25,29,32,41]. After modification, the –OH groups in PBC and SPBC were shifted to 3,413 and 3,415 cm^{-1}, respectively, and the intensity of the –OH vibrational peak was enhanced. The stronger intensity of –OH vibrational peak in SPBC compared to PBC indicated that Na_2HPO_4 increased the amount of –OH groups more effectively [35]. Additionally, the wavenumber of C=O/C=C was altered in PBC and SPBC, which was thought to be due to phosphate modification [2]. Notably, the wavenumber after modification and intensity of the C–O groups were shifted and enhanced, respectively. This phenomenon was even more evident in SPBC. Meanwhile, this suggested that the Na_2HPO_4 modification straw biochar provided more O-containing groups (e.g., hydroxyl and carboxyl groups) [35,36]. Finally, the P–O/P=O groups appeared to vibrate more significantly in PBC and SPBC, which indicated successful phosphate modification [14,29]. Some researchers assumed that –OH, C=O and C–O played a role in the functional group complexation of Cd(II). Furthermore, C=C was thought to be a π-electron donor in the adsorption reaction, facilitating coordination with Cd(II) [4,19,24]. After Cd(II) adsorption, the –OH vibrational peaks on BC, PBC and SPBC were shifted to 3,436; 3,426 and 3,423 cm^{-1}, respectively. Moreover, the intensity of the –OH vibrational peaks changed after Cd(II) adsorption. Nevertheless, the intensity and wavenumber of C–O vibrational peak also changed after adsorption. After the Cd(II) adsorption, the C=O/C=C groups on BC, PBC and SPBC

Table 3
Isotherm model parameters of Cd(II) adsorption

Model	T (°C)		BC	PBC	SPBC
Langmuir	15	q_{max} (mg/g)	37.85	97.90	126.68
		K_L (L/mg)	0.028	0.034	0.129
		R_L	0.105~0.414	0.090~0.374	0.025~0.134
		R^2	0.961	0.985	0.980
		χ^2	0.22	1.75	1.65
		Hybrid fraction	0.84	3.04	0.17
	25	q_{max} (mg/g)	54.55	114.79	154.13
		K_L (L/mg)	0.042	0.063	0.293
		R_L	0.073~0.321	0.050~0.241	0.011~0.064
		R^2	0.942	0.928	0.971
		χ^2	1.02	0.17	39.65
		Hybrid fraction	0.18	0.06	1.52
	35	q_{max} (mg/g)	80.18	133.26	168.64
		K_L (L/mg)	0.044	0.154	0.943
		R_L	0.071~0.314	0.021~0.115	0.004~0.021
		R^2	0.984	0.994	0.992
		χ^2	1.01	0.82	5.58
		Hybrid fraction	0.20	0.10	0.30
Freundlich	15	K_f ($mg^{1-n}·L^n/g$)	12.18	14.19	40.36
		n	5.170	2.944	4.242
		R^2	0.881	0.916	0.788
		χ^2	0.57	9.87	13.78
		Hybrid fraction	1.05	11.83	0.38
	25	K_f ($mg^{1-n}·L^n/g$)	16.54	35.31	52.38
		n	4.788	4.754	4.109
		R^2	0.764	0.761	0.773
		χ^2	3.90	21.92	41.01
		Hybrid fraction	6.51	1.93	9.22
	35	K_f ($mg^{1-n}·L^n/g$)	12.52	47.02	79.02
		n	3.001	4.738	5.802
		R^2	0.897	0.891	0.858
		χ^2	5.03	9.59	23.85
		Hybrid fraction	6.98	7.57	4.46
Temkin	15	b_T (kJ/mol)	1.517×10^3	7.062×10^3	1.157×10^3
		A_T (1/g)	5.917	20.421	22.787
		R^2	0.915	0.960	0.888
		χ^2	46.98	62.74	118.41
		Hybrid fraction	58.72	46.57	52.66
	25	b_T (kJ/mol)	2.324×10^3	1.587×10^3	0.571×10^3
		A_T (1/g)	9.339	18.851	26.553
		R^2	0.825	0.816	0.879
		χ^2	2.75	15.58	28.71
		Hybrid fraction	5.43	6.92	8.71
	35	b_T (kJ/mol)	9.475×10^3	0.679×10^3	0.073×10^3
		A_T (1/g)	17.795	21.286	21.504
		R^2	0.953	0.948	0.938
		χ^2	2.50	4.00	9.68
		Hybrid fraction	4.40	7.71	4.90

were shifted to 1,631; 1,627 and 1,635 cm^{-1}, respectively. According to previous studies, the changes in –OH, C=O and C–O on the sorbent were attributed to complexation with Cd(II) [2,24,30]. Additionally, the change of C=C group was thought to the C=C structure providing π-electrons for Cd(II) adsorption and forming Cd(II)-π interaction with Cd(II) (cation-π interaction) [25,37]. The P–O/P=O group appeared to weaken after adsorption, which suggested that the P–O/P=O group was involved in the Cd(II) adsorption. Wu et al. [24] shown that phosphate in biochar dissolved during adsorption and formed $Cd_3(PO_4)_2$ precipitate in aqueous solution. FTIR analysis shown that O-containing groups in the biochar (e.g., –OH, C=O and C–O) complexed with Cd(II). Cd(II)-π interaction were formed between the C=C structure and Cd(II).

For the XRD analysis of biochars, two broadened peaks appeared at 24.86° and 43.85°, which were considered to be C peak [13,24]. This indicated that the higher graphite content facilitated the interaction of biochar with Cd(II). After adsorption, the intensity of C peaks showed decrease, which could be due to the Cd(II)-π interaction with the graphite structure in biochar [24]. Moreover, new characteristic peaks were found in the adsorbed biochar. The peaks at 2θ = 30.32°, 43.76°, 49.78° and 58.14° were considered to

Table 5
Thermodynamic parameters of Cd(II) removal by biochar

	T (K)	$\Delta G°$ (kJ/mol)	$\Delta H°$ (J·K/mol)	$\Delta S°$ (kJ/mol)
	288	–0.856		
BC	298	–3.044	9.984	34.803
	303	–7.876		
	288	–16.249		
PBC	298	–30.401	49.980	178.680
	303	–52.155		
	288	–45.709		
SPBC	298	–73.683	63.679	237.324
	303	–92.979		

Table 4
Comparison of the Cd(II) adsorption capacity of modified biochar

Sorbent	Condition	q_{max} (mg/g)	References
$KMnO_4$-modified biochar	6.0, 30°C	52.50	[39]
Sulfide-iron decorated biochar	5.5, 45°C	57.71	[40]
Guanidine phosphate-modified biochar	5.0, 30°C	60.30	[23]
Fe_3O_4-modified biochar	6.0, 25°C	92.42	[18]
K_3PO_4-modified biochar	6.0, 25°C	116.00	[35]
SPBC	6.0, 25°C	154.13	This work

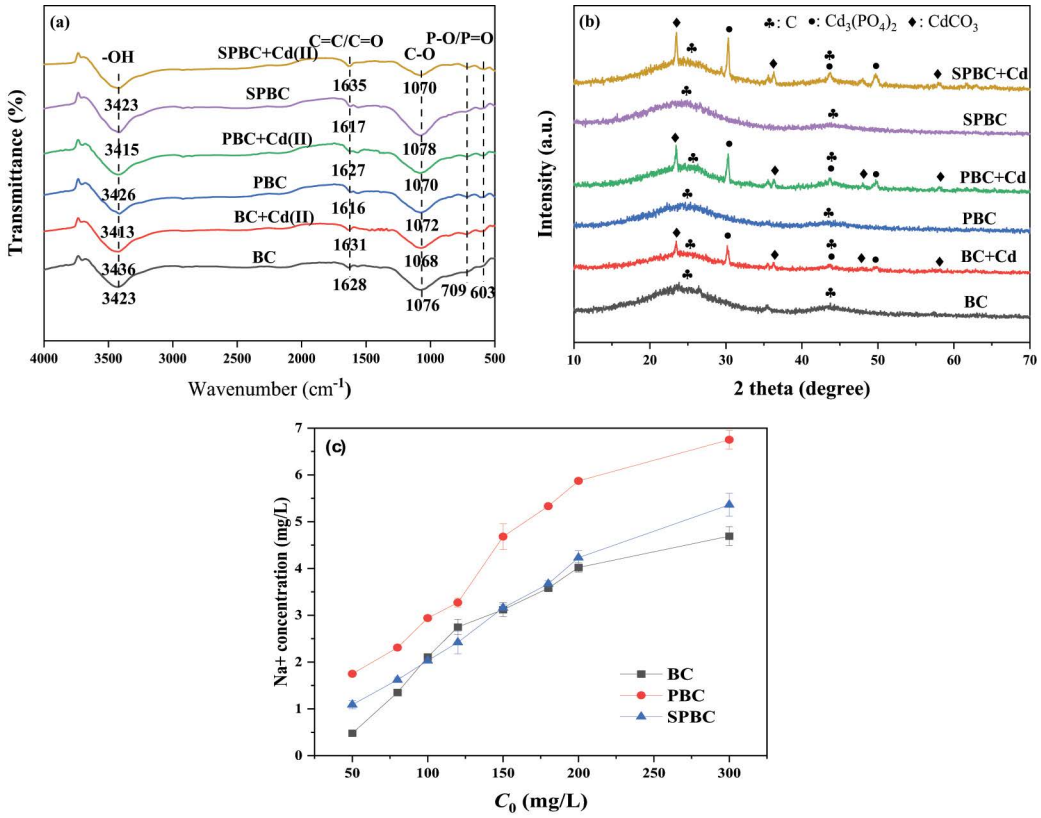

Fig. 6. Fourier-transform infrared spectroscopy and X-ray diffraction analysis of biochar after adsorption. The concentration of Na^+ in the solution (dosage = 25 mg, pH = 6.0, T = 25°C and contact time = 600 min).

be $Cd_3(PO_4)_2$ [2,30]. The peaks at 2θ = 23.52°, 36.36°, 47.93° and 58.16° were $CdCO_3$ [24]. Previous literature has shown that phosphate and carbonic acid in biochar can dissolve in solution and form Cd precipitates in solution, which is also consistent with the results of this paper [14,19,24].

The Na^+ content of solution before and after adsorption (Fig. 6c) was determined at different Cd(II) concentration. The amount of Na^+ released increased with the initial Cd(II) concentration. This indicated that biochars underwent ion exchange during Cd(II) adsorption. As the initial concentration of Cd(II) increased from 50 to 300 mg/L, the Na^+ content of BC, PBC and SPBC increased from 0.48, 1.75 and 1.09 mg/L to 4.69, 6.75 and 5.36 mg/L, respectively. This suggested that the Na^+ in the sorbent provided adsorption sites for Cd(II) adsorption via ion exchange, which was also consistent with previous findings [24,27].

The above analysis shown that the mechanism of Cd(II) removal by BC, PBC and SPBC included the following: (1) complexation between O-containing groups and Cd(II); (2) Cd(II)-π interaction; (3) dissolution of salts (phosphate and carbonate) in the biochar and formation of precipitates with Cd(II); (4) ion exchange between cations in the biochar and Cd(II).

3.9. Cost analysis

The cost of industrial electricity use in Wuhan (China) is 0.08 kW/h. During the preparation of BC, the tube resistance furnace (Power 4 kWh) is used for 2 h. Therefore, the cost of producing 1 kg of BC is 11.65 USD/kg. Moreover, the prices of Na_3PO_4 and Na_2HPO_4 are 0.58 and 0.87 USD/kg, respectively. The total cost of PBC and SPBC was 18.11 and 19.27 USD/kg, respectively. Based on the cost calculation, PBC and SPBC are an inexpensive material.

4. Conclusion

In this work, Na_3PO_4 and Na_2HPO_4 modified straw biochar were used for the Cd(II) adsorption from aqueous solution. Compared to Na_3PO_4 modified biochar, Na_2HPO_4 modified straw biochar possessed more developed pore structure and contained richer O-containing groups. BC, PBC and SPBC shown strong pH dependence for the Cd(II) removal from aqueous solution. K^+, Na^+, Ca^{2+} and Mg^{2+} had little effect on the removal of Cd(II) by biochar, while Cu^{2+} and Pb^{2+} had strong inhibitory effect. The Cd(II) adsorption by biochar was consistent with the pseudo-second-order kinetic model and the Langmuir model, which suggested that the process of Cd(II) removal was homogeneous and chemisorption. The ability of SPBC to remove Cd(II) from aqueous solution faster than BC and PBC was thought to be due to the more abundant adsorption sites of SPBC with well-developed pores. According to the Langmuir model, the theoretical maximum adsorption capacities of BC, PBC and SPBC for Cd(II) were 54.55, 114.79 and 154.13 mg/g, respectively. The removal mechanisms included complexation, ion exchange, Cd(II)-π interaction, electrostatic interaction and co-precipitation. The results indicated that disodium hydrogen phosphate modified biochar had the potential to better treat Cd(II)-containing wastewater.

Funding

This work was supported by National Natural Science Foundation of China (51879099).

Conflicts of interest

The author declared that i have no competing financial interests.

References

[1] L.H. Liu, T.T. Yue, R. Liu, H. Lin, D.Q. Wang, B.X. Li, Efficient absorptive removal of Cd(II) in aqueous solution by biochar derived from sewage sludge and calcium sulfate, Bioresour. Technol., 336 (2021) 125333, doi: 10.1016/j.biortech.2021.125333.
[2] X.P. Li, C.B. Wang, J.N. Tian, J.P. Liu, G.Y. Chen, Comparison of adsorption properties for cadmium removal from aqueous solution by *Enteromorpha prolifera* biochar modified with different chemical reagents, Environ. Res., 186 (2020) 109502, doi: 10.1016/j.envres.2020.109502.
[3] H. Roh, M.R. Yu, K. Yakkala, J.R. Koduru, J.K. Yang, Y.Y. Chang, Removal studies of Cd(II) and explosive compounds using buffalo weed biochar-alginate beads, J. Ind. Eng. Chem., 26 (2015) 226–233.
[4] X.Q. Liu, D.D. Li, J.G. Li, J.L. Wang, S.J. Liang, H. Deng, A novel MnOx-impregnated on peanut shells derived biochar for high adsorption performance of Pb(II) and Cd(II): behavior and mechanism, Surf. Interfaces, 34 (2022) 102323, doi: 10.1016/j.surfin.2022.102323.
[5] Q. Lv, H.X. Wang, M.L. Zhang, J.B. Xue, J. Yang, Synthesis of magnetic biochar/carbonate intercalated Mg-Al layered double hydroxides for enhanced Cd(II) removal from aqueous solution, Desal. Water Treat., 207 (2020) 258–269.
[6] D. Luo, L.Y. Wang, H.Y. Nan, Y.J. Cao, H. Wang, T.V. Kumar, C.Q. Wang, Phosphorus adsorption by functionalized biochar: a review, Environ. Chem. Lett., 21 (2022) 497–524.
[7] K. Huang, C.X. Hu, Q.L. Tan, M. Yu, S. Shabala, L. Yang, X.C. Sun, Highly efficient removal of cadmium from aqueous solution by ammonium polyphosphate-modified biochar, Chemosphere, 305 (2022) 135471, doi: 10.1016/j.chemosphere.2022.135471.
[8] T.T. Yang, Y.M. Xu, Q.Q. Huang, Y.B. Sun, X.F. Liang, L. Wang, X. Qin, L.J. Zhao, Adsorption characteristics and the removal mechanism of two novel Fe-Zn composite modified biochar for Cd(II) in water, Bioresour. Technol., 333 (2021) 125078, doi: 10.1016/j.biortech.2021.125078.
[9] K. Narasimharao, L.P. Lingamdinne, S. Al-Thabaiti, M. Mokhtar, A. Alsheshri, S.Y. Alfaifi, Y.Y. Chang, J.R. Koduru, Synthesis and characterization of hexagonal Mg–Fe layered double hydroxide/grapheme oxide nanocomposite for efficient adsorptive removal of cadmium ion from aqueous solutions: isotherm, kinetic, thermodynamic and mechanism, J. Water Process Eng., 47 (2022) 102746, doi: 10.1016/j.jwpe.2022.102746.
[10] K. Narasimharao, G.K.R. Angaru, Z.H. Momin, S. Al-Thabaiti, M. Mokhtar, A. Alsheshri, S.Y. Alfaifi, J.R. Koduru, Y.Y. Chang, Orange waste biochar-magnesium silicate (OBMS) composite for enhanced removal of U(VI) ions from aqueous solutions, J. Water Process Eng., 51 (2023) 103359, doi: 10.1016/j.jwpe.2022.103359.
[11] Z.Y. Kang, X.G. Jia, Y.C. Zhang, X.X. Kang, M. Ge, D. Liu, C.Q. Wang, Z.X. He, A review on application of biochar in the removal of pharmaceutical pollutants through adsorption and persulfate-based AOPs, Sustainability, 14 (2022) 10128, doi: 10.3390/su141610128.
[12] S.N. Yuan, M.F. Hong, H. Li, Z.X. Ye, H.B. Gong, J.Y. Zhang, Q.Y. Huang, Z.X. Tan, Contributions and mechanisms of components in modified biochar to adsorb cadmium in aqueous solution, Sci. Total Environ., 733 (2020) 139320, doi: 10.1016/j.scitotenv.2020.139320.
[13] M. Zahedifar, N. Seyedi, S. Shafiei, M. Basij, Surface-modified magnetic biochar: highly efficient adsorbents for removal

of Pb(II) and Cd(II), Mater. Chem. Phys., 271 (2021) 124860, doi: 10.1016/j.matchemphys.2021.124860.
[14] G.X. Quan, F.F. Sui, M. Wang, L.Q. Cui, H. Wang, W. Xiang, G.Y. Li, J.L. Yan, Mechanochemical modification of biochar-attapulgite nanocomposites for cadmium removal: performance and mechanisms, Biochem. Eng. J., 179 (2022) 108332, doi: 10.1016/j.bej.2022.108332.
[15] Z.L. Zhang, Y. Li, Y.M. Zong, J. Yu, H. Ding, Y.L. Kong, J.Y. Ma, L. Ding, Efficient removal of cadmium by salts modified-biochar: performance assessment, theoretical calculation, and quantitative mechanism analysis, Bioresour. Technol., 361 (2022) 127717, doi: 10.1016/j.biortech.2022.127717.
[16] L. Zhu, L.H. Tong, N. Zhao, X. Wang, X.X. Yang, Y.Z. Lv, Key factors and microscopic mechanisms controlling adsorption of cadmium by surface oxidized and aminated biochars, J. Hazard. Mater., 382 (2020) 121002, doi: 10.1016/j.jhazmat.2019.121002.
[17] S.H. Zhu, M.K. Irshad, M. Ibrahim, Q. Chen, J.Y. Shang, Q.R. Zhang, The distinctive role of nano-hydroxyapatite modified biochar for alleviation of cadmium and arsenic toxicity in aqueous system, J. Water Process Eng., 49 (2022) 103054, doi: 10.1016/j.jwpe.2022.103054.
[18] D. Lv, Adsorption performance and mechanism of lake sludge-derived ball milling biochar loaded with Fe_3O_4 on Cd(II) in aqueous solution, Desal. Water Treat., 271 (2022) 143–156.
[19] W. Liao, X. Zhang, J.A. Shao, H.P. Yang, S.H. Zhang, H.P. Chen, Simultaneous removal of cadmium and lead by biochar modified with layered double hydroxide, Fuel Process. Technol., 235 (2022) 107389, doi: 10.1016/j.fuproc.2022.107389.
[20] C.A. Pal, L.P. Lingamdinne, Y.Y. Chang, J.R. Koduru, Carbon Dots in Analytical Chemistry, Elsevier, 2023, pp. 161–180.
[21] Q. Miao, G. Li, Potassium phosphate/magnesium oxide modified biochars: interfacial chemical behaviours and Pb binding performance, Sci. Total Environ., 759 (2021) 143452, doi: 10.1016/j.scitotenv.2020.143452.
[22] D.Y. Teng, B.B. Zhang, G.M. Xu, B. Wang, K. Mao, J.X. Wang, J. Sun, X.B. Feng, Z.G. Yang, H. Zhang, Efficient removal of Cd(II) from aqueous solution by pinecone biochar: sorption performance and governing mechanisms, Environ. Pollut., 265 (2020) 115001, doi: 10.1016/j.envpol.2020.115001.
[23] X. Meng, R. Hu, Nitrogen/phosphorus enriched biochar with enhanced porosity activated by guanidine phosphate for efficient passivation of Pb(II), Cu(II) and Cd(II), J. Mol. Liq., 323 (2021) 115071, doi: 10.1016/j.molliq.2020.115071.
[24] J.W. Wu, T. Wang, J.W. Wang, Y.S. Zhang, W.P. Pan, A novel modified method for the efficient removal of Pb and Cd from wastewater by biochar: enhanced the ion exchange and precipitation capacity, Sci. Total Environ., 754 (2021) 142150, doi: 10.1016/j.scitotenv.2020.142150.
[25] Y. Wang, L. Wang, Z.T. Li, D. Yang, J.M. Xu, X.M. Liu, MgO-laden biochar enhances the immobilization of Cd/Pb in aqueous solution and contaminated soil, Biochar, 3 (2021) 175–188.
[26] T. Wang, C. Li, C.Q. Wang, H. Wang, Biochar/MnAl-LDH composites for Cu(II) removal from aqueous solution, Colloids Surf., A, 538 (2018) 443–450.
[27] G.H. Mo, J. Xiao, X. Gao, To enhance the Cd^{2+} adsorption capacity on coconut shell-derived biochar by chitosan modifying: performance and mechanism, Biomass Convers. Biorefin., (2022), doi: 10.1007/s13399-021-02155-9.
[28] X. Tan, W.X. Wei, C.B. Xu, Y. Meng, W.R. Bai, W.J. Yang, A.J. Lin, Manganese-modified biochar for highly efficient sorption of cadmium, Environ. Sci. Pollut. Res., 27 (2020) 9126–9134.
[29] J. Xiang, Q. Lin, X. Yao, G. Yin, Removal of Cd from aqueous solution by chitosan coated MgO-biochar and its in-situ remediation of Cd-contaminated soil, Environ. Res., 195 (2021) 110650, doi: 10.1016/j.envres.2020.110650.
[30] Y.H. Xing, X.S. Luo, S. Liu, W.J. Wan, Q.Y. Huang, W.L. Chen, A novel eco-friendly recycling of food waste for preparing biofilm-attached biochar to remove Cd and Pb in wastewater, J. Cleaner Prod., 311 (2021) 127514, doi: 10.1016/j.jclepro.2021.127514.
[31] Y. Xu, H. Tang, P. Wu, M. Chen, Z. Shang, J. Wu, N. Zhu, Manganese-doped hydroxyapatite as an effective adsorbent for the removal of Pb(II) and Cd(II), Chemosphere, 321 (2023) 138123, doi: 10.1016/j.chemosphere.2023.138123.
[32] B. Tang, H.P. Xu, F.M. Song, H.G. Ge, L. Chen, S.Y. Yue, W.S. Yang, Effect of biochar on immobilization remediation of Cd-contaminated soil and environmental quality, Environ. Res., 204 (2022) 111840, doi: 10.1016/j.envres.2021.111840.
[33] Y. Deng, X.D. Li, F.Q. Ni, Q. Liu, Y.P. Yang, M. Wang, T.Q. Ao, W.Q. Chen, Synthesis of magnesium modified biochar for removing copper, lead and cadmium in single and binary systems from aqueous solutions: adsorption mechanism, Water, 13 (2021) 599, doi: 10.3390/w13050599.
[34] Z.B. Yang, X.C. Liu, M.D. Zhang, L.X. Liu, X.X. Xu, J.R. Xian, Z. Cheng, Effect of temperature and duration of pyrolysis on spent tea leaves biochar: physiochemical properties and Cd(II) adsorption capacity, Water Sci. Technol., 81 (2020) 2533–2544.
[35] Q. Wang, C.J. Duan, C.Y. Xu, Z.C. Geng, Efficient removal of Cd(II) by phosphate-modified biochars derived from apple tree branches: processes, mechanisms, and application, Sci. Total Environ., 819 (2022) 152876, doi: 10.1016/j.scitotenv.2021.152876.
[36] Y.H. Tan, X.R. Wan, X. Ni, L. Wang, T. Zhou, H.M. Sun, N. Wang, X.Q. Yin, Efficient removal of Cd(II) from aqueous solution by chitosan modified kiwi branch biochar, Chemosphere, 289 (2022) 133251, doi: 10.1016/j.chemosphere.2021.133251.
[37] X. He, Z.N. Hong, J. Jiang, G. Dong, H. Liu, R.K. Xu, Enhancement of Cd(II) adsorption by rice straw biochar through oxidant and acid modifications, Environ. Sci. Pollut. Res., 28 (2021) 42787–42797.
[38] C.Q. Wang, H. Wang, Pb(II) sorption from aqueous solution by novel biochar loaded with nano-particles, Chemosphere, 192 (2018) 1–4.
[39] K.Y. Yin, J.Y. Wang, S. Zhai, X. Xu, T.T. Li, S.C. Sun, S. Xu, X.X. Zhang, C.P. Wang, Y.S. Hao, Adsorption mechanisms for cadmium from aqueous solutions by oxidant-modified biochar derived from *Platanus orientalis* Linn leaves, J. Hazard. Mater., 428 (2022) 128261, doi: 10.1016/j.jhazmat.2022.128261.
[40] B. Cao, J.H. Qu, Y.H. Yuan, W.H. Zhang, X.M. Miao, X.R. Zhang, Y. Xu, T.Y. Han, H.J. Song, S.Y. Ma, X. Tian, Y. Zhang, Efficient scavenging of aqueous Pb(II)/Cd(II) by sulfide-iron decorated biochar: performance, mechanisms and reusability exploration, J. Environ. Chem. Eng., 10 (2022) 107531, doi: 10.1016/j.jece.2022.107531.
[41] D.Z. Sun, F.Y. Li, J.W. Jin, S. Khan, K.M. Eltohamy, M.M. He, X.Q. Liang, Qualitative and quantitative investigation on adsorption mechanisms of Cd(II) on modified biochar derived from co-pyrolysis of straw and sodium phytate, Sci. Total Environ., 829 (2022) 154599, doi: 10.1016/j.scitotenv.2022.154599.